Planetary and Space Science 107 (2015) 24–28

Contents lists available at ScienceDirect

Planetary and Space Science

journal homepage: www.elsevier.com/locate/pss

Selective sampling during catastrophic disruption: Mapping the location of reaccumulated fragments in the original parent body

Patrick Michel [a,*], Martin Jutzi [b], Derek C. Richardson [c], Cyrena A. Goodrich [d], William K. Hartmann [d], David P. O'Brien [d]

[a] Laboratoire Lagrange, Université de Nice-Sophia Antipolis, CNRS, Observatoire de la Côte d'Azur, CS 34229, 06304 Nice, Cedex 4, France
[b] Physics Institute, Space Research and Planetary Sciences Center for Space and Habitability, University of Bern, Switzerland
[c] Department of Astronomy, University of Maryland, College Park, MD 20742-2421, USA
[d] Planetary Science Institute, 1700 E. Ft. Lowell, Tucson, AZ 85719, USA

A R T I C L E I N F O

Article history:
Received 12 March 2014
Received in revised form
30 July 2014
Accepted 2 August 2014
Available online 19 August 2014

Keywords:
Asteroids
Collisions
Internal structure
Gravitational reaccumulations

A B S T R A C T

In this paper, we simulate numerically the catastrophic disruption of a large asteroid as a result of a collision with a smaller projectile and the subsequent reaccumulation of fragments as a result of their mutual gravitational attractions. We then investigate the original location within the parent body of the small pieces that eventually reaccumulate to form the largest offspring of the disruption as a function of the internal structure of the parent body. We consider four cases that may represent the internal structure of such a body (whose diameter is fixed at 250 km) in various early stages of the Solar System evolution: fully molten, half molten (i.e., a 26 km-deep outer layer of melt containing half of the mass), solid except a thin molten layer (8 km thick) centered at 10 km depth, and fully solid. The solid material has properties of basalt. We then focus on the three largest offspring that have enough reaccumulated pieces to consider. Our results indicate that the particles that eventually reaccumulate to form the largest reaccumulated bodies retain a memory of their original locations in the parent body. Most particles in each reaccumulated body are clustered from the same original region, even if their reaccumulations take place far away. The extent of the original region varies considerably depending on the internal structure of the parent. It seems to shrink with the solidity of the body. The fraction of particles coming from a given depth is computed for the four cases, which can give constraints on the internal structure of parent bodies of some meteorites. As one example, we consider the ureilites, which in some petrogenetic models are inferred to have formed at particular depths within their parent body.

1. Introduction

In this paper, we investigate the original location within a parent body of small pieces generated by its disruption that eventually reaccumulate to form large aggregates during their escape as a result of their mutual gravitational attraction.

Simulations of a large asteroid catastrophic disruption involving both the fragmentation due to the impact of a projectile, and the gravitational phase during which fragments interact under their mutual attractions, were first performed by Michel et al. (2001). This work as well as subsequent papers (Michel et al., 2001, 2002, 2003, 2004; Durda et al., 2004, 2007; Leinhardt and Stewart, 2009) showed that when a large asteroid is disrupted, the relative velocities between the ejected fragments can still be low enough that they eventually reaccumulate to form gravitational aggregates. The final outcome is a dispersed cluster of gravitational aggregates, each composed of more than one initial fragment, except for the smallest bodies composed of only one of the initial fragments. Their properties match nicely those of representative asteroid families in the main belt when parent bodies similar to those assumed for these families are considered (see e.g., Michel et al., 2001, 2003; Durda et al., 2007).

Michel et al. (2004) started to investigate the original location of pieces composing the largest reaccumulated fragments within the parent body in simulations aimed at reproducing the Koronis asteroid family. The internal structure of the parent body was assumed to be solid monolithic or solid with a small fraction of damaged zones in order to represent a pre-shattered parent body. In the high-impact-energy-regime involved in this particular case, the re-accumulation process lasts up to several days and gives rise to many gravitational encounters before the reaccumulations take place. Thus, it could be expected that such energetic events may cause memory of the initial velocity field to be lost. However, it was found that particles composing the three largest reaccumulated

* Corresponding author.
E-mail address: michel@oca.eu (P. Michel).

http://dx.doi.org/10.1016/j.pss.2014.08.005
0032-0633/

bodies originate from well-clustered regions within the parent body, indicating that re-accumulation is not a random process. Moreover, it was found that the position of the clusters depends greatly on the internal properties of the parent body. This finding is interesting because it may help to constrain the origin scenario of some meteorites for which we can identify the depth at which they must have formed within their parent body. In particular, Michel et al. (2013) suggested that the results of this modeling could be applied to the ureilites, a group of carbon-rich ultramafic achondrites (mantle residues) whose parent body (called Ureilite Parent Body or UPB) is thought to have been disrupted catastrophically early in its history (e.g., Warren and Kallemeyn, 1992; Goodrich, 2004; Downes et al., 2008; Herrin et al., 2010). Some of the properties of ureilites may best be explained if all known samples are derived from a daughter body that formed in this event (Goodrich, 2004; Herrin et al., 2010) rather than directly from the original UPB. Knowing the degree to which that daughter is a select sample of the UPB, and the depth(s) from which that sample is derived, would help to constrain the petrologic structure of the UPB and therefore models of ureilite petrogenesis. However, Warren (2012) argued that the modeling by Michel et al. (2004) was not relevant to the UPB breakup because only solid parent bodies were considered, whereas the UPB is inferred to have been partly molten at the time of breakup.

In this paper, we simulate numerically the catastrophic disruption of a large asteroid in various states of melting, in order to assess the influence of those states on the original locations of pieces composing the three largest reaccumulated bodies. The diameter of the parent body is considered to be 250 km. In Section 2, we briefly describe our numerical method. In Section 3 we describe the various internal structures that we consider for this study. Section 4 presents the results. A discussion and conclusions are given in Section 5.

2. Numerical method

Our numerical approach has already been described in various papers (see e.g., Michel et al., 2002, 2004). It consists of performing the simulations in two phases. First, the fragmentation phase is computed using a 3D SPH hydrocode (Benz and Asphaug, 1994; Jutzi et al., 2008) in which several fragmentation models were introduced and validated. Then the gravitational phase, in which fragments reaccumulate, is computed using the collision-enabled version of the parallel *N*-body code `pkdgrav` (Richardson et al., 2000) that allows computing the interaction of millions of particles by detecting their collisions and modeling their reaccumulations. Reaccumulations take place when two particles collide with each other at a relative speed smaller than their mutual escape speed; in that case they are merged into a single object whose mass is the sum of the mass of the two particles and whose velocity is that of the center of mass of the two particles. Otherwise, particles bounce with normal and tangential coefficients of restitution set to 0.5 (moderate energy dissipation) and 1 (no surface contact coupling), respectively.

When fragmentation is over, the output of the SPH simulation, i.e., the positions, densities, masses and velocities of particles that represent the generated fragments, are fed into the *N*-body code that follows the gravitational evolution and reaccumulation of generated fragments. During this phase, the paths taken by the particles from their original positions in the parent body to their final ones in reaccumulated bodies are tracked. We can thus determine the original depths within the parent of the particles forming the reaccumulated bodies. This is the first time this investigation has been performed for various internal structures, instead of just solid ones. We focus on the three largest reaccumulated bodies in order to have enough reaccumulated particles to consider.

3. Internal structures of the parent body

In this study, because we are interested in its potential application to the Ureilite Parent Body, we consider the following four kinds of internal structures:

1. Fully molten.
2. Half molten by mass (molten outer layer, 26 km thick).
3. Solid except for a molten layer, 8 km thick, centered at 10 km depth (10% of asteroid mass).
4. Fully solid.

For the solid, we use material properties of basalt, although basalt may not be the best analogue of mantle material composing the Ureilite Parent body. However, we consider this material because a successful comparison between SPH simulations and high-speed impact experiments on basalt targets was performed (Benz and Asphaug, 1994), allowing us to validate the code with this material. In contrast, within the molten bodies or layers, the fragmentation phase is purely hydrodynamical (meaning no deviatoric stresses are considered).

The number of SPH particles representing the 250 km-diameter parent body is 800,000. The minimum particle size limited by the numerical resolution is thus 3 km.

4. Results

In each case, the simulations consider an 84 km-diameter projectile impacting at 5 km/s at a 45° angle into the parent body. These somewhat arbitrary initial conditions are chosen to lead to a largest reaccumulated body whose mass is at least 10% of the mass of the parent body. Therefore, we limit our investigation to highly disruptive cases in which the mass gets distributed into many small reaccumulated fragments instead of just a few. These cases are very different from the cratering regime, which will be the subject of another investigation.

4.1. Molten parent body

The fraction of mass of the molten parent body in the first-, second- and third-largest reaccumulated bodies is 0.1, 0.06, and 0.04, respectively. These three bodies are all aggregates (reaccumulated fragments). Fig. 1 shows the original location of particles composing these three reaccumulated bodies in the original parent body in a 3D cross section. These regions are quite narrow but essentially go from one side of the body to the other. None of these reaccumulated fragments contain particles that come solely from a particular or very narrow range of depth. More precisely, particles come from the same extended region (i.e., there are no particles that come from an area disconnected from the others), but not from a given depth.

As an exercise, we quantified the fraction of particles coming from a given zone, fixed between 30 and 40 km depth. The percentage of particles coming from this zone is essentially the same for each of the three reaccumulated bodies (about 10–12%). We also computed the mass distributions as a function of original depth (Fig. 2). We used a bin size of 2 km and the curves are normalized by the mass of the corresponding fragment. One can see that the particles in each of the daughter bodies cover essentially the entire depth within the parent body, as could be seen qualitatively in Fig. 1.

4.2. Half-molten parent body

In the case of a parent body 50% of whose the mass is molten, the fraction of mass in the first-, second-and third-largest reaccumulated bodies is 0.1, 0.07, and 0.06, respectively, which is not drastically different from what was found for the fully molten parent body. However, the original location of particles composing these fragments is different from that in the case of the fully molten body (see Fig. 3). For instance, the fraction of particles coming from the zone between 30 and 40 km depth in the third largest fragment is about 29%, while it was about 12% in the fully molten case. In particular, we find that the particles composing the third-largest fragment come from a region of the parent body that is clustered between 20 and 70 km depth (see Fig. 2).

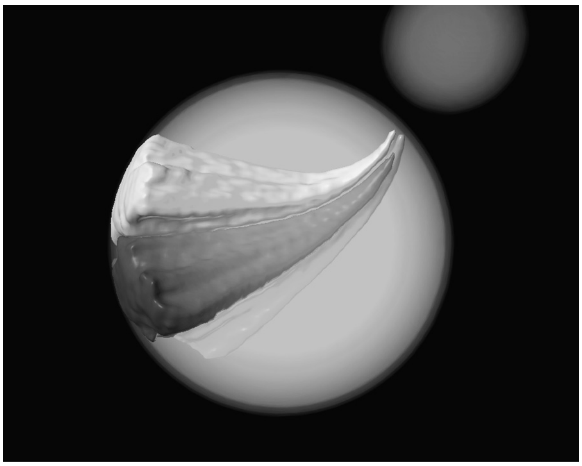

Fig. 1. 3D image of the original positions of particles that will reaccumulate and form the largest, second, and third largest fragments (called F1, F2, F3, in decreasing size in Fig. 2) in increasing darkness (blue, yellow and red in the on-line color version) from a molten parent body. The impactor is shown at the top right and moves vertically down. In the investigated greatly disruptive regimes, all the material that is not in these largest fragments (i.e., the largest fraction of the parent body) is blown away, i.e., it will not reaccumulate (or only in very small fragments).

4.3. Solid parent body with a thin molten layer

We consider here the case of a solid parent body containing a molten layer that has 10% of the total mass, located at 10 km-depth. In this case, the fraction of mass in the first-, second-and

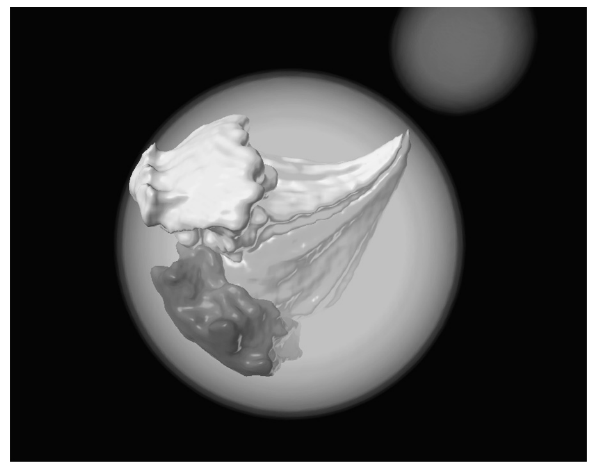

Fig. 3. Same as Fig. 1 for a half-molten parent body.

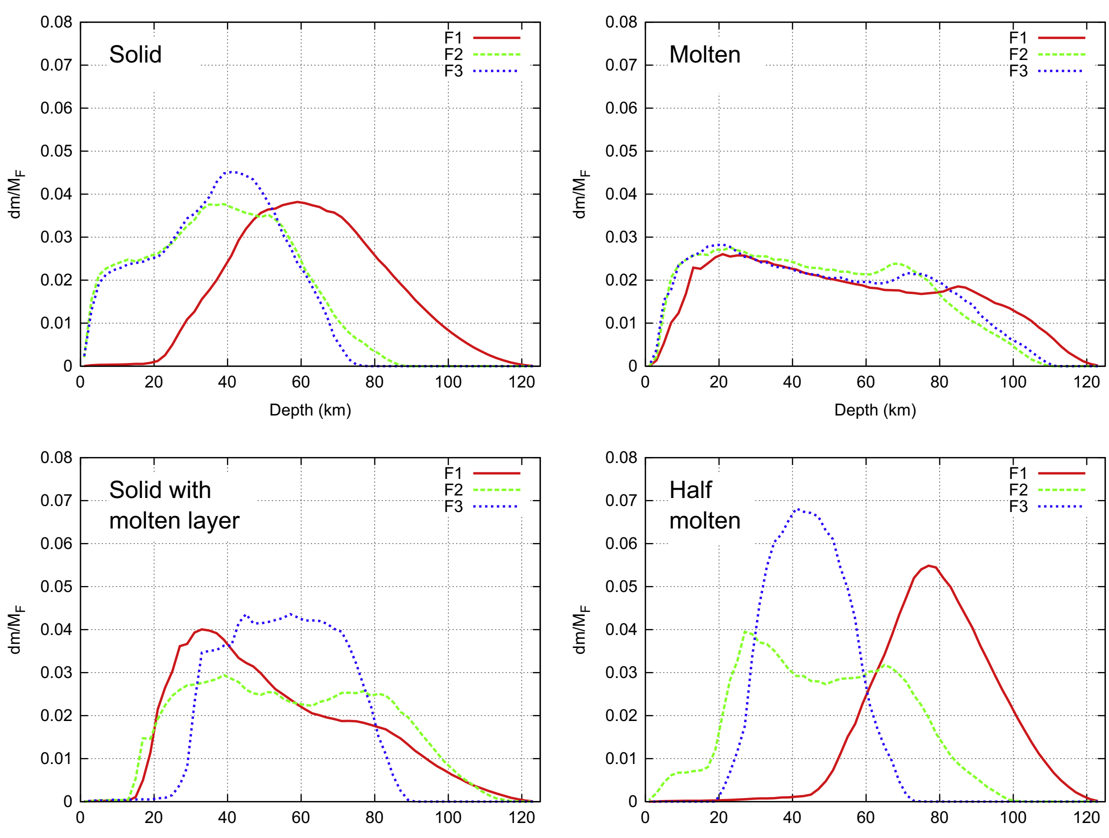

Fig. 2. Fraction of mass contained in the three largest reaccumulated bodies (F1, F2, F3, in decreasing size), as a function of original depth within the parent body for the four considered internal structures. Bin size is 2 km and curves are normalized by the mass of the corresponding body.

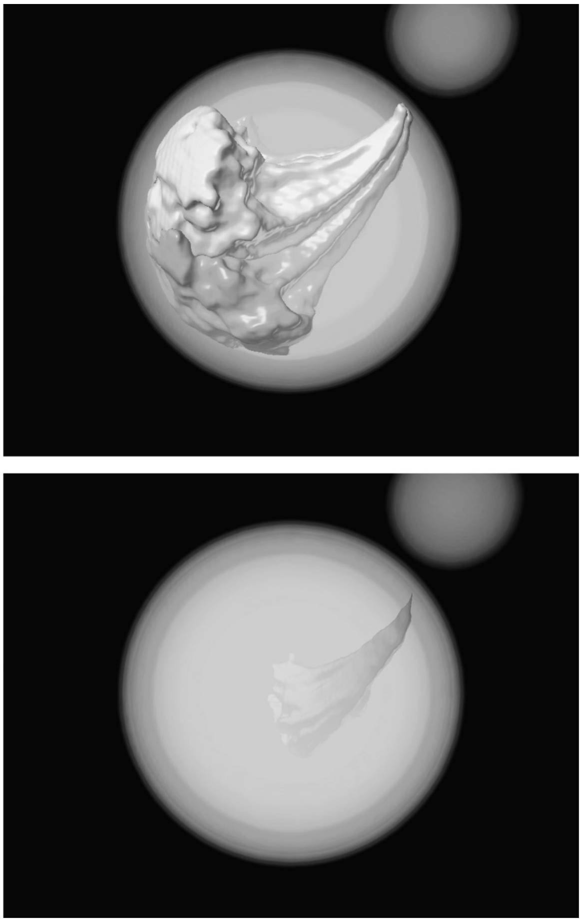

Fig. 4. Same as Fig. 1 for a solid parent body with a thin molten layer (10% of the total mass) at 10 km depth. The second image shows the third largest fragment (F3 in Fig. 2) that is not visible on the first image in which it is behind the first and second largest fragments (F1 and F2 in Fig. 2).

third-largest reaccumulated bodies is 0.2, 0.07, and 0.02, respectively, which is quite different (at least for the first and third) than for a half-molten body. Note that the third-largest reaccumulated body now contains particles from a more restricted region, namely between 20 and 90 km depths (see Fig. 2). Since the mass that ultimately comprises the third largest reaccumulated body is very small, it is hidden behind the other colored regions in Fig. 4.

4.4. Fully solid parent body

The fraction of mass in the first-, second- and third-largest reaccumulated bodies of the fully solid parent body is 0.23, 0.08, and 0.05, respectively. The fraction of original mass in the largest reaccumulated body is thus about twice that for the cases of molten or half-molten bodies, but not that different from the solid body with a thin molten layer. This shows that a solid body is more resistant to impact than a molten or half-molten body due to the absence of tensile strength in the latter cases. Moreover, as can be seen in Fig. 5, the original locations of particles constituting the largest reaccumulated bodies shrink compared to those in the molten or half-molten cases. However, the second- and third-largest offsprings have about 20% of their mass coming from the zone between 30 and 40 km depth, which is 10% less than in the case of the half-molten parent body, but still higher than in the case of a fully molten body. Thus, each of the three largest reaccumulated bodies preferentially samples distinct regions (depths) of the parent (as predicted by Michel et al., 2004) with detailed differences depending on amount and location of melt.

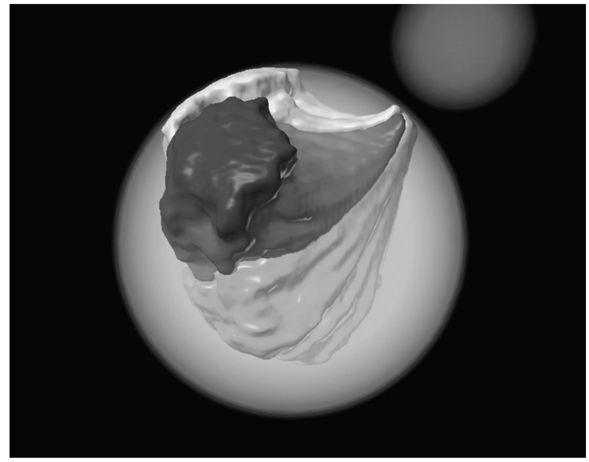

Fig. 5. Same as Fig. 1 for a solid parent body.

5. Discussion and conclusions

We simulated the disruption of parent bodies whose internal structure contains various degrees and locations of melt. We then tracked the original location in the parent body for particles that ended up in the three largest reaccumulated bodies. Our results show that in the highly disruptive investigated cases, these reaccumulated bodies sample distinct regions (ranges of depths) of the parent, with detailed differences depending on the amount and location of the melt. On the other hand, when the parent body is fully molten, then the sampled region goes through the whole body and does not preferentially sample any particular depth.

These results have interesting implications for origin scenarios of meteorites whose original depth in their parent body can be estimated. For instance, our results in terms of depths of derivation in the parent body of the material in the offspring bodies can be compared with the predictions from petrologic modeling of ureilite meteorites (i.e., depths of derivation of ureilites in various petrogenetic models). There are two main competing petrogenetic models for ureilites. The so-called smelting model (Walker and Grove, 1993; Singletary and Grove, 2003; Goodrich et al., 2007 provides strong constraints on the depth of derivation (i.e., the depth of their final, high–temperature equilibration) of ureilites in their parent body, as a function of their mafic mineral Fe/Mg composition (i.e., Fo of olivine). The most recent calculated depth distributions from 232 main group ureilites (Michel et al., 2013) show that the majority of ureilites must have been derived from a limited range of depths around 18 km, assuming a UPB of 428 km diameter (the estimated parent body size constrained by smelting as in Wilson et al. (2008) and assuming a small metallic core). We note that these estimates for the size of the UPB and depths of derivation in the smelting model differ from previous estimates (Wilson et al., 2008; Hartmann et al., 2011), due mainly to adopting new ideas for the density (Warren, 2012) and thermal properties (Wilson and Keil, 2013) of the cold, non-heat conductive outer shell. At 5 Ma after CAI (the inferred time of breakup of the UPB: Kita et al., 2003; Goodrich et al., 2010), the UPB probably had a near–solid mantle ($<0.2\%$ melt), with a layer of melt that was ≈ 1.4 km thick, at ≈ 6 km depth (Wilson et al., 2008). Therefore, the case of the solid target with a molten layer considered here is most relevant to the UPB, even if all characteristics are not exactly the same. From Fig. 2, one can see that the three largest reaccumulated bodies all derive the majority (peak) of their material from greater depths (between ≈ 30 and 60 km) than those represented by ureilites as suggested in the smelting model. They also derive most of the rest of their material from deeper than the peak, whereas most of the rest of the ureilites are derived from shallower depths, according to the smelting model. A better match of peak depthsmight be obtained with a slightly smaller asteroid (e.g., 90 km radius), but this slight change in target size might not change the result that the rest of the material in the fragment is derived from deeper depth than the peak. On the other hand, the currently estimated size of the UPB in the smelting model is actually significantly greater than the one considered in this study (and could have been even larger, if no metallic core was present). Thus, the specific results presented in this work do not constitute a definitive test of the smelting model for ureilites.

The competing model, broadly called the nebular inheritance model, provides fewer constraints on depths of origin of ureilites, but most likely requires larger UPB sizes. It also permits (but does not require) ureilites to be derived from deeper in the UPB. Thus, if the results of our numerical modeling of disruption remain similar for larger parent bodies, they could be consistent with the nebular inheritance model.

So far our numerical modeling of catastrophic disruptions has explored only a small part of parameter space but already has given us interesting results concerning the influence of the internal structure on the original location of particles constituting the largest reaccumulated bodies. They show that this modeling has the potential to test the degree to which a group of meteorites is a selective sample of their original parent body, and to test competing petrogenetic models that predict their original depths of formation. We have illustrated this for the case of the ureilites, although we stress that we have not yet modeled sufficiently large parent bodies to reach any definitive conclusions with respect to ureilites. In a future work, we will consider larger targets in order to check whether our results still apply to the ureilites, as well as test a wider range of impact parameters (impactor mass, velocity, impact angle) to better understand the range of selective sampling that can occur during large impacts.

One particular region of parameter space that merits further study is the transitional regime between regular cratering impacts and full catastrophic disruption. One could visualize transitional, sub-catastrophic, super-cratering parameter combinations (e.g., low-speed, large impactors) where a portion of the outer layers of the target are ejected (as in cratering) but where the ejections speeds are slow enough to allow reassembly of escaping debris. Such reassembly/escape combinations may plausibly produce daughter asteroids that represent more restricted outer regions of the target than we have found in the catastrophic disruption model described in this paper. We plan investigations of this transitional super-cratering impact regime to check whether the outcomes in such regimes can reconcile with different petrogenic models for the UPB.

Acknowledgments

P.M. acknowledges support from the French space agency CNES. This work was also supported by NASA OSS Grant no. #NNX12AI84G and NASA Cosmochemistry Grant no. #NNX12AH74G, as well as NASA PG&G Grant no. #NNX08AM39G and NSF Grant no. #AST1009579.

References

Benz, W., Asphaug, E., 1994. Impact simulations with fracture. I—method and tests. Icarus 107 (January), 98.

Downes, H., Mittlefehldt, D.W., Kita, N.T., Valley, J.W., 2008. Evidence from polymict ureilite meteorites for a disrupted and re-accreted single ureilite parent asteroid gardened by several distinct impactors. Geochim. Cosmochim. Acta 72 (October), 4825–4844.

Durda, D.D., Bottke, W.F., Enke, B.L., Merline, W.J., Asphaug, E., Richardson, D.C., Leinhardt, Z.M., 2004. The formation of asteroid satellites in large impacts: results from numerical simulations. Icarus 170 (July), 243–257.

Durda, D.D., Bottke, W.F., Nesvorný, D., Enke, B.L., Merline, W.J., Asphaug, E., Richardson, D.C., 2007. Size-frequency distributions of fragments from SPH/N-body simulations of asteroid impacts: comparison with observed asteroid families. Icarus 186 (February), 498–516.

Goodrich, C., 2004. Ureilitic breccias: clues to the petrologic structure and impact disruption of the ureilite parent asteroid. Chem. der Erde/Geochem. 64 (Nov.), 283–327.

Goodrich, C.A., Goldstein, J., Kita, N.T., Mikouchi, T., Zolensky, M., Herrin, J., Ash, R.D., McDonough, W.F., Jenniskens, P.M., 2010. Metal in ureilitic fragments of Almahata Sitta. Meteorit. Planet. Sci. Suppl. 73 (September), 5319.

Goodrich, C.A., Van Orman, J.A., Wilson, L., 2007. Fractional melting and smelting on the ureilite parent body. Geochim. Cosmochim. Acta 71 (June), 2876–2895.

Hartmann, W.K., Goodrich, C.A., O'Brien, D.P., Michel, P., Weidenschilling, S.J., Sykes, M.V., March 2011. Breakup and reassembly of the ureilite parent body, formation of 2008 TC3/almahata sitta, and delivery of ureilites to earth. In: Lunar and Planetary Institute Science Conference Abstracts. Lunar and Planetary Institute Science Conference Abstracts, vol. 42, p. 1360.

Herrin, J.S., Zolensky, M.E., Ito, M., Le, L., Mittlefehldt, D.W., Jenniskens, P., Ross, A.J., Shaddad, M.H., 2010. Thermal and fragmentation history of ureilitic asteroids: insights from the Almahata Sitta fall. Meteorit. Planet. Sci. 45 (October), 1789–1803.

Jutzi, M., Benz, W., Michel, P., 2008. Numerical simulations of impacts involving porous bodies. I. Implementing sub-resolution porosity in a 3D SPH hydrocode. Icarus 198 (November), 242–255.

Kita, N.T., Ikeda, Y., Togashi, S., Shimoda, G., Morishita, Y., Weisberg, M.K., 2003. Evolution of ureilites by ^{26}Al heating of the parent body. Geochim. Cosmochim. Acta Suppl. 67 (September), 220.

Leinhardt, Z.M., Stewart, S.T., 2009. Full numerical simulations of catastrophic small body collisions. Icarus 199 (February), 542–559.

Michel, P., Benz, W., Richardson, D.C., 2003. Disruption of fragmented parent bodies as the origin of asteroid families. Nature 421 (February), 608–611.

Michel, P., Benz, W., Richardson, D.C., 2004. Catastrophic disruption of pre-shattered parent bodies. Icarus 168 (April), 420–432.

Michel, P., Benz, W., Tanga, P., Richardson, D.C., 2001. Collisions and gravitational reaccumulation: forming asteroid families and satellites. Science 294 (November), 1696–1700.

Michel, P., Benz, W., Tanga, P., Richardson, D.C., 2002. Formation of asteroid families by catastrophic disruption: simulations with fragmentation and gravitational reaccumulation. Icarus 160 (November), 10–23.

Michel, P., Goodrich, C.A., Jutzi, M., Wilson, L., O'Brien, D.P., Hartmann, W.K., Weidenschilling, S.J., March 2013. Numerical modeling of catastrophic disruption of molten and partly molten asteroids, with implications for breakup of the ureilite parent body. In: Lunar and Planetary Institute Science Conference Abstracts. Lunar and Planetary Institute Science Conference Abstracts, vol. 44, p. 1300.

Richardson, D.C., Quinn, T., Stadel, J., Lake, G., 2000. Direct large-scale N-body simulations of planetesimal dynamics. Icarus 143 (January), 45–59.

Singletary, S.J., Grove, T.L., 2003. Early petrologic processes on the ureilite parent body. Meteorit. Planet. Sci. 38 (Jan.), 95–108.

Walker, D., Grove, T., 1993. Ureilite smelting. Meteoritics 28 (December), 629–636.

Warren, P.H., 2012. Parent body depth-pressure-temperature relationships and the style of the ureilite anatexis. Meteorit. Planet. Sci. 47 (Feb.), 209–227.

Warren, P.H., Kallemeyn, G.W., 1992. Explosive volcanism and the graphite-oxygen fugacity buffer on the parent asteroid(s) of the ureilite meteorites. Icarus 100 (November), 110–126.

Wilson, L., Goodrich, C.A., Van Orman, J.A., 2008. Thermal evolution and physics of melt extraction on the ureilite parent body. Geochim. Cosmochim. Acta 72 (December), 6154–6176.

Wilson, L., Keil, K., 2013. Fast melt production and easy melt migration in differentiated asteroids implies giant sills not, magma oceans. LPI Contrib. 1768 (October), 8004.